

Data Repository Item (2 appendices) for Kidwell, Best, & Kaufman “Taphonomic trade-offs”

Appendix 1. Additional information on dated shells and dating methods.

Figure DR1. Extent of glutamic acid (Glu) racemization in ^{14}C -dated mollusks calibrated (cal yr BP) assuming a 450 yr marine reservoir effect. Linear regression (line) based on 12 shells from the modern shelf defines the calibrated age equation for other shells analyzed in this study. The form of the calibration curve (scaling along the y-axis) is based on a parabolic model (Mitterer and Kriausakul, 1989). Data listed in Table DR1.

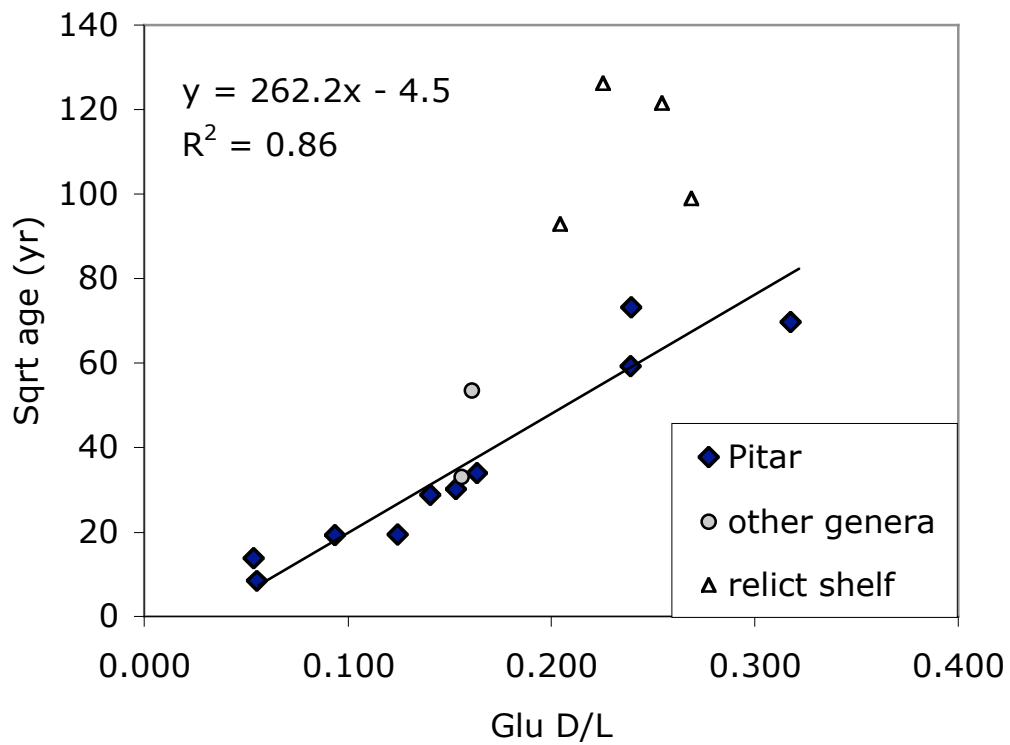


Figure DR2. Homogeneity of shell ages (log scale) as a function of depth in sedimentary column. Shells were extracted by sieving increments of the sedimentary column, hence the plotting of both upper and lower limits to original shell position. Shell ages are known only to $\sim\pm 50$ years at best, and thus all dates $< \sim 50$ yr should be collapsed into a single age bin. Virtually all dated shells are from the upper 25 cm of surface sediments. Down-core changes in sediment mass properties suggest that bioturbation is most intense within the top 10–12 cm of the column, although open water-filled burrows were detected to ~ 70 cm (maximum core length recovered from San Blas area during project). The age homogeneity of shells within the top 25 cm verifies that this entire interval is within the mixing zone, although typically only the top 1–2 mm of sediment is oxidized.

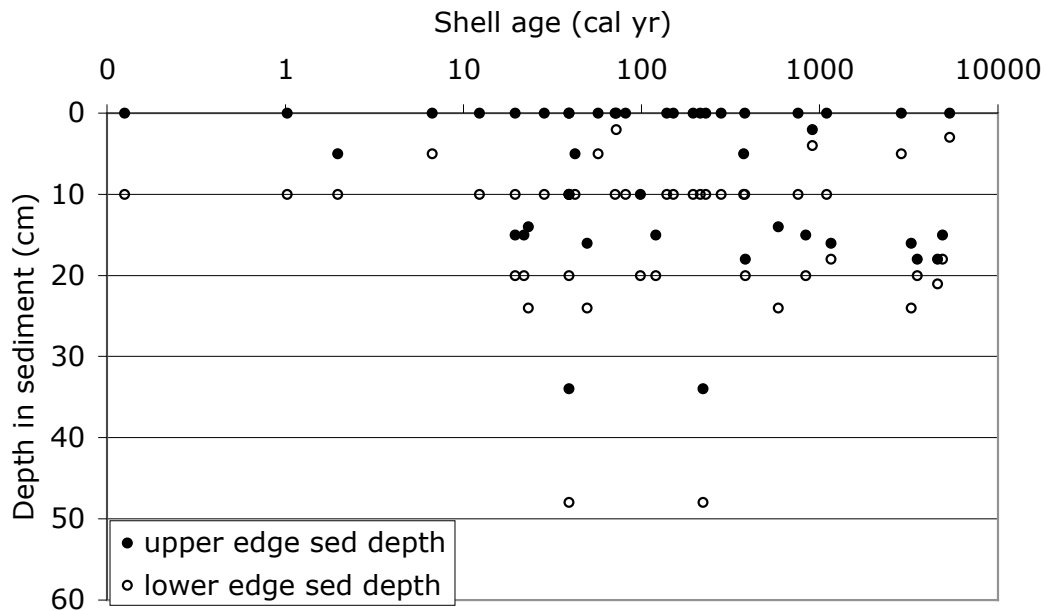


Table DR1 – Summary information for all dates from the modern San Blas Archipelago, Caribbean Panama (inboard of modern reef front), plus 4 dated *Pitar* shells from the relict San Blas shelf (seaward of modern reef front) and 4 dated *Pitar* shells (Glu data only) from mixed-composition sediments at the foot of patch reefs in Bocas del Toro, Caribbean Panama. This table is 4 landscape pages long and 4 landscape pages wide.

Table 1. Summary information for all dates from modern shelf of San Blas Archipelago, Panama (inboard of modern reef front), plus additional calibrated dates for relict shelf of San Blas (seaward of reef front) and from Bocas del Toro, Panama

Note: Table 1 is 4 landscape pages deep and 4 landscape pages wide, followed by footnotes in portrait pages

sediment type	Shell Identification Number of (Kidwell, Chicago)	Identification number for field location	Location name in fieldnotes	Latitude	Longitude	Water Depth (m)
carbonate mud	RC17	95SB050	Pico Feo deep CO3 box Shell RC 17	09-33.22 N	78-58.08 W	9
carbonate mud	RC20a	95SB050	Pico Feo deep CO3 box Shell RC 20a	09-33.22 N	78-58.08 W	9
carbonate mud	RC23	97UC010	Cruise 97-10 Lemon Cay grab 2 Shell RC 23	09-32.29 N	78-54.34 W	42
carbonate mud	RC24	97UC010	Cruise 97-10 Lemon Cay grab 3 Shell RC 24	09-32.29 N	78-54.34 W	42
carbonate mud	RC27	97SB058	Nudibranch Lagoon 97SB058 (Guigalatupo)	09-32.78 N	78-58.18 W	3
carbonate mud	RC28	97SB058	Nudibranch Lagoon 97SB058 (Guigalatupo)	09-32.78 N	78-58.18 W	3
carbonate mud	RC29	97SB058	Nudibranch Lagoon 97SB058 (Guigalatupo)	09-32.78 N	78-58.18 W	3
carbonate mud	RC30	97SB058	Nudibranch Lagoon 97SB058 (Guigalatupo)	09-32.78 N	78-58.18 W	3
carbonate mud	RC37	97UC022	Cruise 97-22 near Lemon Cay grab #1	09-31.10N	78-54.25 W	44
carbonate mud	RC46	97UC022	Cruise 97-22 near Lemon Cay grab #1	09-31.10N	78-54.25 W	44
carbonate mud	RC61	97SB058	Nudibranch Lagoon 97SB058 (Guigalatupo)	09-32.78 N	78-58.18 W	3

carbonate mud	RC62	97SB058	Nudibranch Lagoon 97SB058 (Guigalatupo)	09-32.78 N	78-58.18 W	3
carbonate grassbed	RC25	97SB056	Russ Meyer 97SB056 (grassbed behind Pico Feo)	09-33.23 N	78-58.18 W	5
carbonate grassbed	RC25A	97SB056	Russ Meyer 97SB056 (grassbed behind Pico Feo)	09-33.23 N	78-58.18 W	5
carbonate grassbed	RC26	97SB056	Russ Meyer 97SB056 (grassbed behind Pico Feo)	09-33.23 N	78-58.18 W	5
carbonate grassbed	RC43	97SB056	Russ Meyer 97SB056 (grassbed behind Pico Feo)	09-33.23 N	78-58.18 W	5
carbonate grassbed	RC44	97SB056	Russ Meyer 97SB056 (grassbed behind Pico Feo)	09-33.23 N	78-58.18 W	5
carbonate grassbed	RC45	97SB056	Russ Meyer 97SB056 (grassbed behind Pico Feo)	09-33.23 N	78-58.18 W	5
reef/hardground	RC50	97SB050	Pico Feo mini-transect Reef top facies II	09-33.22 N	78-58.08 W	1
reef/hardground	RC21	97UC030	Cruise 97-30 Green Island Box 1 Shell RC 21	09-29.20 N	78-38.20 W	30
reef/hardground	RC49	97SB050	Pico Feo mini-transect Reef top facies II	09-33.22 N	78-58.08 W	1
reef/hardground	RC51	97SB050	Pico Feo mini-transect Reef top facies I	09-33.22 N	78-58.08 W	1
reef/hardground	RC52	97SB050	Pico Feo mini-transect Reef top facies III	09-33.22 N	78-58.08 W	1
reef/hardground	RC53	97SB050	Pico Feo mini-transect Reef top facies III	09-33.22 N	78-58.08 W	1
siliciclastic mud	RC1	95SB054	Soledad Redux Shell RC1	09-25.78 N	78-54.11 W	9
siliciclastic mud	RC2	95SB054	Soledad Redux Shell RC2	09-25.78 N	78-54.11 W	9
siliciclastic mud	RC3	95SB054	Soledad Redux Shell RC3	09-25.78 N	78-54.11 W	9

siliciclastic mud	RC4	95SB054	Soledad Redux Shell RC4	09-25.78 N	78-54.11 W	9
siliciclastic mud	RC13	97UC003	Cruise 97-03 Rio Agua mud Box Shell RC 13	09-28.70 N	79-01.00 W	35
siliciclastic mud	RC14	97UC003	Cruise 97-03 Rio Agua mud Box Shell RC 14	09-28.70 N	79-01.00 W	35
siliciclastic mud	RC15	97UC003	Cruise 97-03 Rio Agua mud Box Shell RC 15	09-28.70 N	79-01.00 W	35
siliciclastic mud	RC16	97UC003	Cruise 97-03 Rio Agua mud Box Shell RC 16	09-28.70 N	79-01.00 W	35
siliciclastic sandy	RC5	97UC025	Cruise 97-25 Rio Azucar Box 2 Shell RC 5	09-26.00 N	78-38.60 W	10
siliciclastic sandy	RC6	97UC025	Cruise 97-25 Rio Azucar Box 2 Shell RC 6	09-26.00 N	78-38.60 W	10
siliciclastic sandy	RC7	97UC025	Cruise 97-25 Rio Azucar Box 2 Shell RC 7	09-26.00 N	78-38.60 W	10
siliciclastic sandy	RC8	97UC025	Cruise 97-25 Rio Azucar Box 2 Shell RC 8	09-26.00 N	78-38.60 W	10
siliciclastic sandy	RC9	97UC006	Cruise 97-06 Rio Agua exp. Site Box 2 Shell RC 9	09-27.12 N	79-00.16 W	9
siliciclastic sandy	RC11	97UC006	Cruise 97-06 Rio Agua exp. Site Box 2 Shell RC 11	09-27.12 N	79-00.16 W	9
siliciclastic sandy	RC12	97UC006	Cruise 97-06 Rio Agua exp. Site Box 2 Shell RC 12	09-27.12 N	79-00.16 W	9
mixed composition mud	RC39	95SB053, 3-8	Mango Inlet mini-transect 95SB053 site 3-8 (Ulagsukun)	09-33.02 N	78-59.73 W	10
mixed composition mud	RC48	95SB053, 3-8	Mango Inlet mini-transect 95SB053 site 3-8 (Ulagsukun)	09-33.02 N	78-59.73 W	10
mixed composition peri- reefal	RC40	95SB053, 13-8	Mango Inlet mini-transect 95SB053 site 13-8 (Ulagsukun)	09-33.02 N	78-59.73 W	4
mixed composition peri- reefal	RC41	95SB053, 7-8	Mango Inlet mini-transect 95SB053 site 7-8 (Ulagsukun)	09-33.02 N	78-59.73 W	6

mixed composition peri-reefal	RC42	95SB053, 7-8	Mango Inlet mini-transect 95SB053 site 7-8 (Ulagsukun)	09-33.02 N	78-59.73 W	6
mixed composition peri-reefal	RC47	95SB053, 13-8	Mango Inlet mini-transect 95SB053 site 13-8 (Ulagsukun)	09-33.02 N	78-59.73 W	4

Relict shelf of San Blas

reef/hardground	RC31	97UC016	Cruise 97-16 Soledad Shelf	09-37.13 N	78- 52.06 W	74
mixed composition mud	RC32	97UC018	Cruise 97-18 Soledad Shelf	09-37.30 N	78-52.00 W	110
mixed composition mud	RC33	97UC020	Cruise 97-20 Soledad Shelf	09-37.48 N	78-52.13 W	170
mixed composition mud	RC34	97UC021	Cruise 97-21 Soledad Shelf	09-37.40 N	78-51.90 W	150

Modern Lagoon of Bocas del Toro area

mixed composition peri-reefal	RC56	97UC051	Cruise 97-51 Bocas area, behind Zapamillos	09-16.51 N	82-06.35 W	15
mixed composition peri-reefal	RC57	97UC051	Cruise 97-51 Bocas area, behind Zapamillos	09-16.51 N	82-06.35 W	15
mixed composition peri-reefal	RC58	97UC051	Cruise 97-51 Bocas area, behind Zapamillos	09-16.51 N	82-06.35 W	15
mixed composition peri-reefal	RC59	97UC051	Cruise 97-51 Bocas area, behind Zapamillos	09-16.51 N	82-06.35 W	15
mixed composition peri-reefal	RC60	97UC051	Cruise 97-51 Bocas area, behind Zapamillos	09-16.51 N	82-06.35 W	15

Sample type	Depth in sediment from which shell collected	Species name	Taxonomic Code for project (University of Chicago)	Shell weight (initial, dry; mg)	Shell height (umbo to commissure; mm)	NMDS taphonomic Dimension 1 [shell damage state]	NMDS taphonomic Dimension 2 [shell damage state]	Notes on shell condition
box core	0-2 cm	Pitar fulminatus (Menke)	96	100	17	-0.95	0.349	
box core	18-20 cm	Pitar sp	70	30	16	-1.70	-0.339	
grab #2	0-10 cm	Pitar arestus (Dall & Simpson)	23	20	9.3	0.64	-0.104	
grab #3	0-10 cm	Pitar arestus (Dall & Simpson)	23	30	9.7	0.99	0.017	
pvc push core #4	0-5 cm	Macoma (Austromacoma) constricta (Brugiere)	113	20	10	0.87	-0.417	
grab	0-10 cm	Pitar cf P. fulminatus (Menke)	96	100	8.5	0.78	0.042	
pvc push core #4	34-48 cm	Pitar cf P. fulminatus (Menke)	96	170	8.5	-0.02	-0.043	gall
pvc push core#4	34-48 cm	Macoma (Austromacoma) constricta (Brugiere)	113	10	9	0.15	-0.239	
grab #1	0-10 cm	Pitar cf P. arestus (Dall & Simpson)	23	190	10.5	0.34	-0.064	dendritic pattern on shell exterior
grab #1	0-10 cm	Pitar albidus (Gmelin)	137	20	9.8	0.47	0.036	interesting shell, black in structure
pvc push core#4	14-24 cm	Macoma sp.	xx	30	6.6	1.21	0.264	

pvc push core#4	14-24 cm	Pitar cf <i>P. fulminatus</i> (Menke)	96	70	11	-0.82	-1.319	green algae
incubation box core	0-10 (8-10?)	Pitar cf <i>P. fulminatus</i> (Menke)	96	150	8	0.30	0.145	exterior surface partly chalky and pitted
grab; Ds 247	0-10 cm	Pitar cf <i>P. fulminatus</i> (Menke)	96	80	12	0.99	-0.44	
porewater box core	16-24 cm	Pitar cf <i>P. fulminatus</i> (Menke)	96	110	13	0.63	-0.063	
incubation box core	10-20 cm	Pitar sp	70	50	13	0.48	-0.113	
incubation box core	10-20 cm	Pitar sp	70	30	13.5	1.01	0.148	
porewater box core	16-24 cm	Pitar albidus (Gmelin)	137	20	7.2	0.29	0.386	
grab # II E	0-10 cm	Codakia (Ctena) sp	99	90	11	0.58	-0.01	
box core	0-5 cm	Callista eucymata (Dall)	138	330	12	-1.46	1.047	approx. width, fragment
grab # II E	0-10 cm	Codakia (Ctena) sp	99	100	6	1.34	0.185	
grab # I A	0-10 cm	Codakia (Ctena) sp	99	130	10	0.40	0.45	
grab # III G	0-10 cm	Codakia (Ctena) sp	99	190	13.5	-0.01	0.34	cemented grains on surface
grab # III G	0-10 cm	Codakia (Ctena) sp	99	100	7.5	-1.43	-0.403	high surface alteration; biogenic (root etching?)
porewater box core	0-2 cm	Pitar arestus (Dall & Simpson)	23	230	7	0.94	0.068	
porewater box core	2-4 cm	Pitar arestus (Dall & Simpson)	23	30	8.1	0.19	0.198	cemented grains on surface
porewater box core	16-18 cm	Pitar albidus (Gmelin)	137	60	11	0.37	-0.118	

porewater box core	18-20 cm	Pitar arestus (Dall & Simpson)	23	170	12	0.20	-0.555
box core	0-5 cm	Pitar albidus (Gmelin)	137	10	5.9	0.89	0.174
box core	5-10 cm	Pitar arestus (Dall & Simpson)	23	150		1.31	-0.103
box core	15-20 cm	Pitar sp	23	100		1.62	0.108
box core	15-20 cm	Pitar sp	23	80		0.81	0.172
box core #2	5-10 cm	Pitar albidus (Gmelin)	137	30	9	0.17	-0.094
box core #3	5-10 cm	Pitar albidus (Gmelin)	137	30	9	0.55	-0.151
box core #4	15-20 cm	Pitar arestus (Dall & Simpson)	23	110	5.7	0.44	-0.178
box core #5	15-20 cm	Pitar arestus (Dall & Simpson)	23	130	12.5	0.53	-0.056
box core #6	0-3 cm	Pitar arestus (Dall & Simpson)	23	40	10	0.28	-0.2
box core #7	15-18 cm	Pitar arestus (Dall & Simpson)	23	200		0.29	-0.044
box core #2	18-21 cm	Pitar arestus (Dall & Simpson)	23	70	9.4	-0.12	-0.423
Ds118, shell #2357	0-10 cm	Pitar cf P. arestus (Dall & Simpson)	23	270	13	0.13	0.093
grab #3-8, shell #5482	0-10 cm	Pitar cf P. fulminatus (Menke)	96	250	13.5	1.00	0.058
grab #13-8, shell #6927	0-10 cm	Pitar cf P. arestus (Dall & Simpson)	23	120	15	-1.74	-0.28
grab #7-8, shell #4995	0-10 cm	Pitar cf P. fulminatus (Menke)	96	180	9	-1.02	-0.029

choose
 between this
 and 20 for
 analysis

grab #7-8, shell #4999	0-10 cm	Pitar cf P. fulminatus (Menke)	96	130	11	-1.41	-0.001
grab #13-8, shell #6992	0-10 cm	Pitar cf P. fulminatus (Menke)	96	60	12	-1.43	-0.091
grab #3	0-10 cm	Pitar albidus (Gmelin)	137	20	10	-0.81	0.162
grab #1	0-10 cm	Pitar cf P. fulminatus (Menke)	96	50	9	-0.86	0.209
grab #2	0-10 cm	Pitar cf P. fulminatus (Menke)	96	40	8	-1.69	0.041
grab #1	0-10 cm	Pitar cf P. fulminatus (Menke)	96	100	13.2	-1.71	0.074
box core	6-9 cm	Pitar cf P. arestus (Dall & Simpson)	23	540	7.6	-0.13	0.223
box core	9-12 cm	Pitar cf P. arestus (Dall & Simpson)	23	340	11.2	0.38	0.066
box core	9-12 cm	Pitar cf P. arestus (Dall & Simpson)	23	410	7.8	-1.57	-0.16
box core	30-33 cm	Pitar cf P. arestus (Dall & Simpson)	23	190	11.3	-0.15	0.41
box core	30-33 cm	Pitar cf P. arestus (Dall & Simpson)	23	190	9.5	0.34	-0.064

opaque
section in
shell
structure

opaque
section in
shell
structure

Shell Identification Number of (Kidwell, Chicago)	Shell Identification Number for Amino Acid UAL (Kaufman)	ASP D/L	GLU D/L	SER	ALA	ILE	Shell Identification Number of (Kidwell, Chicago)	Shell Identification Number of Tucson AMS C-14	DC_13VAL UE
RC17	2882	0.151	0.050				RC17	AA34579	1.36
RC20a	2883	0.296	0.125				RC20a	AA34580	1.76
RC23	2885	0.165	0.054				RC23	AA34582	M
RC24	2886	0.153	0.055				RC24	AA34583	1.26
RC27	3193	0.154	0.046	0.431		0.047	RC27	AA38904	2.12
RC28	3194	0.186	0.073	0.488	0.086	0.062	RC28		
RC29	3192	0.178	0.074	0.462	0.098	0.068	RC29	AA38905	1.36
RC30	3195	0.149	0.041	0.331	0.042	0.046	RC30	AA38906	1.43
RC37	3253	0.124	0.041	0.355	0.031	0.056	RC37		
RC46	3254	0.174	0.062	0.476	0.080	0.081	RC46		
RC61	3196	0.123	0.036	0.304	0.034	0.052	RC61		

RC62	3197	0.233	0.110	0.598	0.171	0.094	RC62		
RC25	3224	0.103	0.038	0.300	0.039	0.043	RC25		
RC25A	3228	0.116	0.041	0.298	0.046	0.042	RC25A		
RC26	3232	0.127	0.044	0.382	0.042	0.059	RC26		
RC43	3223	0.144	0.055	0.409	0.051		RC43		
RC44	3226	0.116	0.041	0.322	0.037	0.053	RC44		
RC45	3230	0.404	0.235	0.310	0.471	0.259	RC45		
RC50	3236	0.211	0.031				RC50		
RC21	2884	0.368	0.161				RC21	AA34581	2.29
RC49	3235	0.204	0.034	0.171	0.022	0.032	RC49	AA38907	0.7
RC51	3237	0.168	0.052	0.165	0.046	0.064	RC51	AA38908	0.07
RC52	3238	0.075	0.021	0.034	0.367	0.024	RC52	AA38909	2.17
RC53	3239	0.547	0.156	0.498	0.279	0.138	RC53	AA38910	0.32
RC1	2867	0.048	0.019				RC1	AA34565	0.76
RC2	2868	0.319	0.153				RC2	AA34566	1.44
RC3	2869	0.334	0.164				RC3	AA34567	1.56

RC4	2870	0.371	0.239				RC4	AA34568	1.69
RC13	2878	0.07	0.027				RC13		
RC14	2879	0.135	0.042				RC14	AA34576	0.81
RC15	2880	0.153	0.059				RC15	AA34577	1.92
RC16	2881	0.115	0.034				RC16	AA34578	0.83
RC5	2871	0.063	0.023				RC5	AA34569	0.32
RC6	2872	0.262	0.094				RC6	AA34570	M
RC7	2873	0.105	0.035				RC7	AA34571	0.88
RC8	2874	0.325	0.141				RC8	AA34572	1.85
RC9	2875	0.379	0.240				RC9	AA34573	1.15
RC11	2876	0.441	0.318				RC11	AA34574	1.4
RC12	2877	0.442	0.275				RC12		
RC39	3240	0.206	0.092	0.474	0.149	0.148	RC39		
RC48	3241	0.042	0.019	0.031	0.009	0.040	RC48		
RC40	3242	0.257	0.122	0.358	0.272	0.174	RC40		
RC41	3244	0.159	0.064	0.426	0.071	0.494	RC41		

RC42	3245	0.170	0.081	0.210	0.105	0.238	RC42		
RC47	3243	0.198	0.075	0.321	0.112	0.203	RC47		
RC31	3199	0.324	0.205	0.181	0.364	0.351	RC31	AA38900	1.43
RC32	3198	0.415	0.269	0.272	0.511	0.541	RC32	AA38901	1.24
RC33	3200	0.431	0.255	0.335	0.578	0.540	RC33	AA38902	1.25
RC34	3201	0.368	0.226	0.263	0.433	0.268	RC34	AA38903	2.1
RC56	3227	0.313	0.148	0.529	0.278	0.132	RC56		
RC57	3231	0.146	0.058	0.365	0.065	0.056	RC57		
RC58	3229	0.351	0.194	0.337	0.385	0.235	RC58		
RC59	3225	0.331	0.149	0.596	0.303	0.173	RC59		
RC60	3233	0.140	0.056	0.380	0.068	0.049	RC60		

Fraction of Modern	age (14C yr)	±	min cal age with delta R = 0	max cal age with delta R = 0	mid point of 1 sigma calibrated age range	± half range	square root of age (yr)	GLU AGE = calib age based on regression of Glu D/L vs sqrt age (yr)	Calibrated age (yrs)
0.9495+-0.0050	415	40						72	72
0.9113+-0.0048	745	40	335	429	382	47	19.54482029		382
0.9337+-0.0049	550	40	142	249	195.5	53.5	13.98213145		195.5
0.9409+-0.0049	490	40	0	142	71	71	8.426149773		71
0.9523+-0.0040	393	33						57	57
								214	214
0.9466+-0.0055	440	45						222	222
0.9568+-0.0052	355	43						39	39
								39	39
								138	138
								23	23

									586	586
									28	28
									39	39
									50	50
									98	98
									39	39
									3263	3263
									12	12
0.6794+-0.0040	3105	45	2811	2924	2867.5	56.5	53.54904294			2867.5
1.1195+-0.0067 post-bomb									20	20
0.9549+-0.0059	370	49							81	81
1.0954+-0.0091 post-bomb									1	1
0.8258+-0.0041	1538	39	1047	1141	1094	47	33.07567082			1094
1.0952+-0.0059 post-bomb									0	0
0.8435+-0.0050	1365	45	870	958	914	44	30.23243292			914
0.8201+-0.0049	1595	45	1104	1213	1158.5	54.5	34.03674485			1158.5

								280	280
								230	230
0.3625+-0.0026	8151	56	8535	8725	8630	95	93		8630
0.3196+-0.0024	9163	60	9593	9957	9775	182	99		9775
0.1990+-0.0020	12968	78	14298	15249	14773.5	475.5	122		14773.5
0.1804+-0.0019	13758	81	15691	16175	15933	242	126		15933
								1177	1177
								112	112
								2150	2150
								1195	1195
								104	104

Footnotes to Table DR1:

Shell identification numbers: each dated shell has a lab ID number for the University of Chicago (RC prefix), one assigned by the AMS facility in Tucson (AA prefix), and one assigned by the amino acid racemization lab at Northern Arizona University (UAL). One half of each shell was submitted for AAR analysis, and the other half either submitted for AMS 14C analysis or archived in Chicago.

Identification numbers for field locations of Best (2000): prefix 97UC denotes sampling site during cruise of RV *Uracca* in 1997; prefixes 95SB and 97SB denote sampling site during scuba work from San Blas station in 1995 or in 1997.

Sample type: Porewater and incubation box cores (15 cm x 25 cm) were taken by divers and penetrated to ~20 cm maximum in the sediment column; these were excavated in 2-cm increments (1997 field work at STRI San Blas research station with Tim Ku & Lynn Walter). Ship-deployed box cores (1997 cruise of RV *Uracca*) had dimensions 50 cm x 50 cm and penetrated the seafloor to ~50 cm maximum, and were excavated in 5 cm increments. PVC push cores were diver emplaced, 4 inches in diameter, and excavated in 5 cm increments. Grab samples were either hand-scoops by divers (to ~10 cm depth in sediment) or, during the 1997 cruise, collected using a Petersen sampler (estimated 10 cm penetration).

Amino Acid Racemization: Values for Interlaboratory Comparative Standards (ILC, Wehmiller, 1984) for Asp are: ILC-A = 0.393 ± 0.006 ; ILC-B = 0.686 ± 0.011 ; ILC-C = 0.824 ± 0.028 ; and for Glu: ILC-A = 0.205 ± 0.009 ; ILC-B = 0.424 ± 0.009 ; ILC-C = 0.849 ± 0.010 . Asp = aspartic acid; Glu = glutamic acid. See further comments below.

References cited in Appendix 1:

Mitterer, R. M., and Kriausakul, N., 1989, Calculation of amino acid racemization ages based on apparent parabolic kinetics: *Quaternary Science Reviews*, v. 8, p. 353-358.

Wehmiller, J. F., 1984, Interlaboratory comparison of amino acid enantiomeric ratios in fossil Pleistocene mollusks: *Quaternary Research*, v. 22, p. 109-120.

Appendix 2. Additional information on taphonomic analyses.

Taphonomic half-life and recycling rates.-- Skewed distributions of shell ages like those we have found in San Blas (Fig. 1 in main text) occur in age-dated molluscan death assemblages elsewhere, and suggest a decline in shell loss over time, assuming a constant rate of shell input. An exponential fit (Chi-square, $p = 0.002$) yields an estimated “taphonomic half-life” of 520 years (*sensu* Staff et al., 1986; the time interval over which 50% of specimens are destroyed by post-mortem processes). This can be construed as a conservative estimate of the overall recycling rate for large (≥ 6 mm) molluscan shells in the modern San Blas shelf system.

Outlier date from modern shelf.—One *Pitar* shell from sandy grassbeds (RC45) yielded a calibrated age of ~3300 years based on Glu D/L, and is treated as an outlier because it lies far above the next oldest shell dated from carbonate grassbeds (maximum age ~100 cal yrs, $N = 6$) as well as outside carbonate soft-sediments as a group (maximum age ~600 cal yrs, $N = 18$; see Figures 1 and 2 in main text). All tests are robust to inclusion or exclusion of this outlier: it does not affect the significance of extreme value differences between siliciclastic and all carbonate dates, nor between siliciclastics and carbonate soft-sediments (Table DR2). It is not included in the analysis of damage accrual with time (Figure 2 in main text).

Table DR2. Exact probabilities for observed exceedences in shell ages, both with and without including the outlier date shell (RC45) from carbonate grassbeds.

Sets of dates being compared	n of first set (N of second set)	Oldest date in first set	Exceedences in second set	probability of those exceedences
all carbonate dates wo/outlier versus siliciclastics	27 (17)	2900	4	0.0175
all carbonate dates w/outlier versus siliciclastics	28(17)	3300	4	0.0160
carbonate soft-sediments versus reefs	17(10)	600	3	0.0410
reefs versus siliciclastics	10(17)	2900	4	0.1347
carbonate soft-sediments wo/outlier versus siliciclastics	17(17)	600	7	0.0036
carbonate soft-sediments	18(17)	3300	4	0.0454

w/outlier versus siliciclastics				
all muds versus all sands	22(13)	3500	3	0.0437

Comment on extreme value statistics.—Extreme value statistics make no assumption about the shape of the frequency distribution or sampling protocol, but simply establishes the probability, for each value in a ranked series, of a new value being lower or higher (Denny and Gaines, 2000; Gumbel, 1958). The resolution of the method depends solely on the size of the existing sample. To calculate probabilities, known values are ranked in descending order: the most extreme upper value (here, maximum age of dated shells) would be given rank 18 if the total N of dated shells is 18, and the lowest value (youngest dated shell) would be given rank 1. The probability (p) of the next newly dated shell being *younger* than the oldest already known is simply the rank of the oldest known shell (18) divided by the total sample size plus 1 (19), and thus is 0.95. There is thus a 0.05 probability that the next dated shell will be *older*. This can be repeated for any value in a ranked series, and series can be compared even if their sample sizes are different. Probabilities of next finding a younger shell (= 1 - probability of finding an older shell) are plotted in Figure DR3A for sedimentary settings.

An exact probability can also be calculated that a particular number (1, 2, 3, etc) of values in the second set exceeds the highest value observed in the first set (“exceedences”; Kinnison, 1985). This is:

$$\text{prob} = (n * C[N,x]) / ((N+n) * C[N+n-1, x]),$$

where n is the size of the first set, N the size of the second set, x the number of exceedences in the second set, and $C[N,x] = N! / (x!(N-x)!)$. These values are reported in Table DR2. The probability that 4 siliciclastic dates will be older than those from all carbonates is 0.016 if the outlier grassbed date (RM45) is included, and 0.018 if it is excluded, thus has no effect on the significance of the difference. Reef shell ages are significantly older than those from carbonate soft-sediments (muds, sandy grassbeds) at $p = 0.041$, and siliciclastics shells are older than those from carbonate soft-sediments at $p = 0.004$ (0.045 if outlier grassbed shell is included). Siliciclastic shells are not significantly different from reef shells ($p = 0.135$).

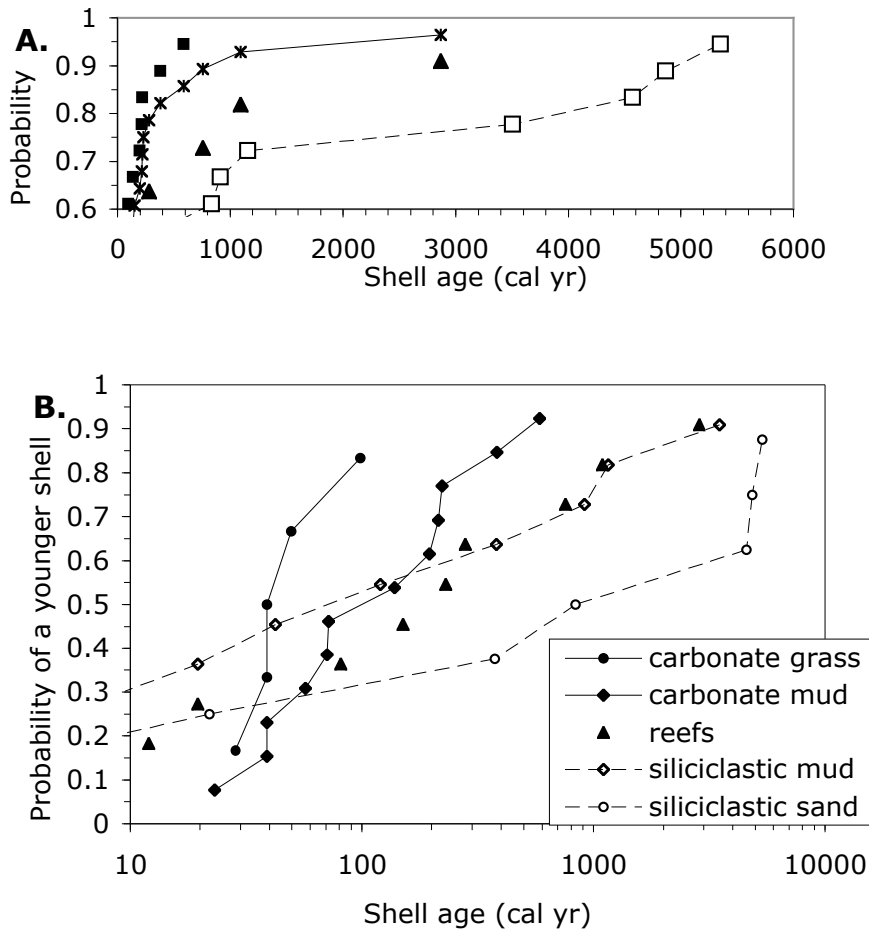


Figure DR3. A. Based on extreme value analysis, maximum shell ages in siliciclastic sediments (open squares) are significantly greater than in carbonate environments (asterisks), and is also higher than in non-reefal carbonate muds and sandy grassbeds (black squares). B. Because of smaller sample sizes, statistical power is lost (maximum probability falls below 0.95, marked by horizontal line) if data are partitioned to test for grain size effects within sediment composition types. The relative positions of curves suggest, however, that grain size explains far less of the variation in maximum shell ages than does sediment composition.

Comment on variation in shell age with sediment composition.— Although maximum shell age was the *de facto* operational definition of “magnitude of time-averaging” in early studies, workers have begun to use a variety of metrics of central tendency and dispersion to characterize and differentiate (modern) time-averaged assemblages. Not all of these descriptors are appropriate for highly skewed distributions such as found in time-averaged assemblages (e.g., standard deviation and interquartile range), but are included here for completeness (Table DR3). Also, with the exception of maximum shell age, none of these can be formally tested unless sampling is random, which it usually is not (because of limits on funds available for testing shells). However, for comparison with other studies, the siliciclastic and carbonate median shell ages in Table DR3 are not significantly different (nonparametric medians test, $p = 0.26$), which is not surprising given the low N, nor are the shapes of the distributions detectably different (nonparametric Kolmogorov Smirnov test, $p > 0.10$), but the differences are consistent with the ranking of facies by extreme value analysis.

Given the consistency in sampling procedure and the similar numbers of shells available among facies, the observed differences in these other measures probably signify meaningful variation in time-averaging within the modern San Blas shelf system as a function of sediment composition. All measures yield the same ranking of the 3 facies, and the magnitudes of the differences between end-member siliciclastic and carbonate facies are striking, especially given the small sample sizes (~2-fold differences in maximum and median shell ages and standard deviation, ~3-fold difference in half-lives, and ~20-fold differences in quartile ranges). This contrasts with erratic results using these same metrics when data are partitioned according to sediment grain size rather than sediment composition (see next comment).

Table DR3. Summary descriptive statistics for dated shells grouped according to sediment grain size. Ages in calendar years.

Table 3. Summary statistics for dated shells grouped according to sediment grain size. Ages in calendar years.

	N	mean	standard deviation	variance	median	minimum	maximum	25th %	75th %	inter-quartile range	semi-quartile range	estimated half-life
All dated shells	45	738	1395	1947084	120	0	5354	39	586	547	273.5	520
Sediment Type												
all carbonates (reef & nonreef)	24	401	857	734063	71.5	1	3263	39	218	179	89.5	272
siliciclastics	15	1453	2016	4065090	375	0	5354	20	3506	3486	1743	1000
mixed composition	6	300	258	66367	255	0	756	151	380	229	114.5	
Grain Size												
all muds	22	372	763	583165	96	0	3506.5	39	380	763.6	382	
sands including grassbeds	13	1503	2148	4614210	98	2	5354.5	39	3263	2148	1074	
reefs, aprons, & hardgrounds	10	549	890	792820	190.5	1	2867.5	20	756	890.4	445.2	

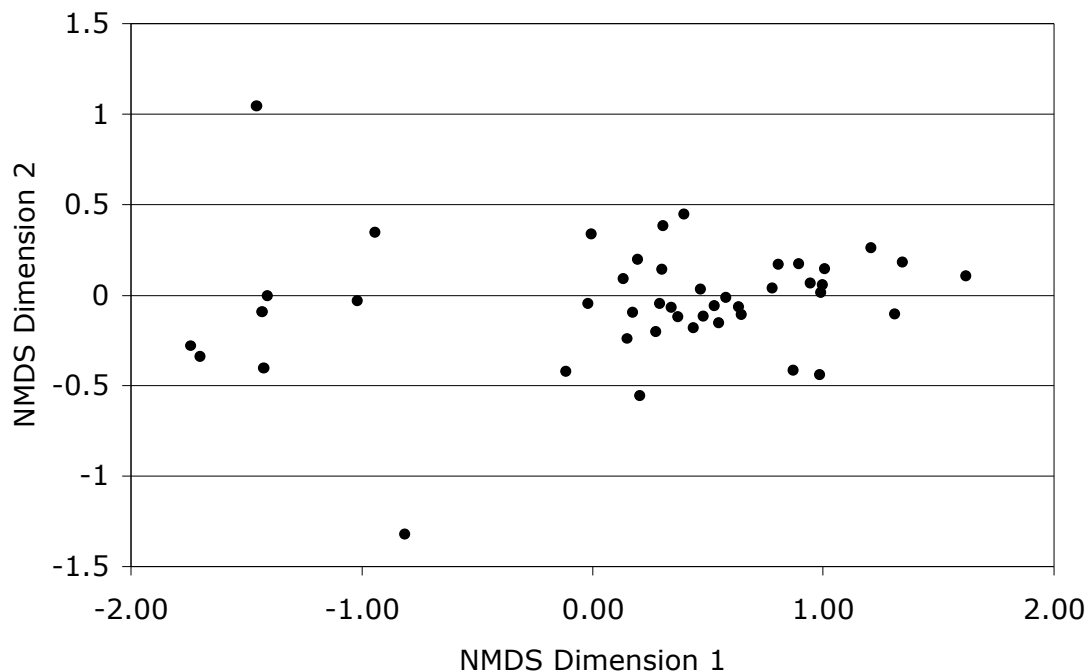
Comment on variation in shell age with sediment grain size.-- Sorting dated shells according to sediment grain-size rather than sediment-composition reveals no detectable variation (Table DR3). Within the siliciclastic facies belt, sands yielded older maximum and median shell ages than muds (median 255 versus 190 years; see raw data in Table DR1), probably due to greater potential for physical reworking and mixing in the higher-energy sand settings, but the differences are not significant. Among carbonate samples, sediments intimately associated with reefs (pockets within framework or debris at the foot of a reef) yielded the oldest shells (~1100 and 2900 cal yrs; Table 1). However, the median shell-age from reefal carbonate sediments was the same as in non-reefal carbonate sediments (50 vs 72 years), suggesting that time-averaged rates of destruction are comparably high in both kinds of carbonate habitats. The incorporation of some relatively old shells in reefal sediments should not be surprising: rare deep reworking by storms and mass wastage could exhume older shells and redeposit them either onto the reef-flat or into reef cavities at various positions down-slope, injecting them into otherwise rapidly degrading (short half-life) assemblages.

Using extreme value statistics, shell ages from sands (siliciclastic and carbonate data pooled) are significantly greater than from muds ($p = 0.044$), but only as a one-tailed test. Because there is no a priori reason to expect that sands would have greater time-averaging (more frequent physical reworking might promote greater time-averaging via winnowing, but should also promote shell destruction), a two-tailed test is more appropriate (resulting in loss of significance). Thus sediment grain size seems to have less of a correlation with maximum shell age than does sediment composition.

Comment on scoring of taphonomic damage.— All dated shells were disarticulated but entire (unbroken). Damage variables were generally scored only for shell interior surfaces to insure that they were post-mortem, and were observed using 10x magnification. Variables included degree of rounding of commissural edge; color (ranged from slight beige discoloration associated with microbial maceration, to brown and green from algae, and gray, black and orange from mineral precipitates in siliciclastics); fine-scale alteration (requiring SEM to distinguish chemical, microbial, or abrasive origins) inside the pallial line, outside the pallial line, and of the muscle scar

(these are usually different microstructures); bioerosion by roots (etching), clionid sponges, “worms”, undifferentiated microborings, and predatory damage from gastropods and crabs; bioencrustation by serpulids, other worms, calcareous algae, foramifera, and bryozoans. Both dimensions of the 2-D NMDS analysis are plotted in Figure DR4 below.

Figure DR4. Two-dimensional plot of results of shell damage analysis, all San Blas dated shells.

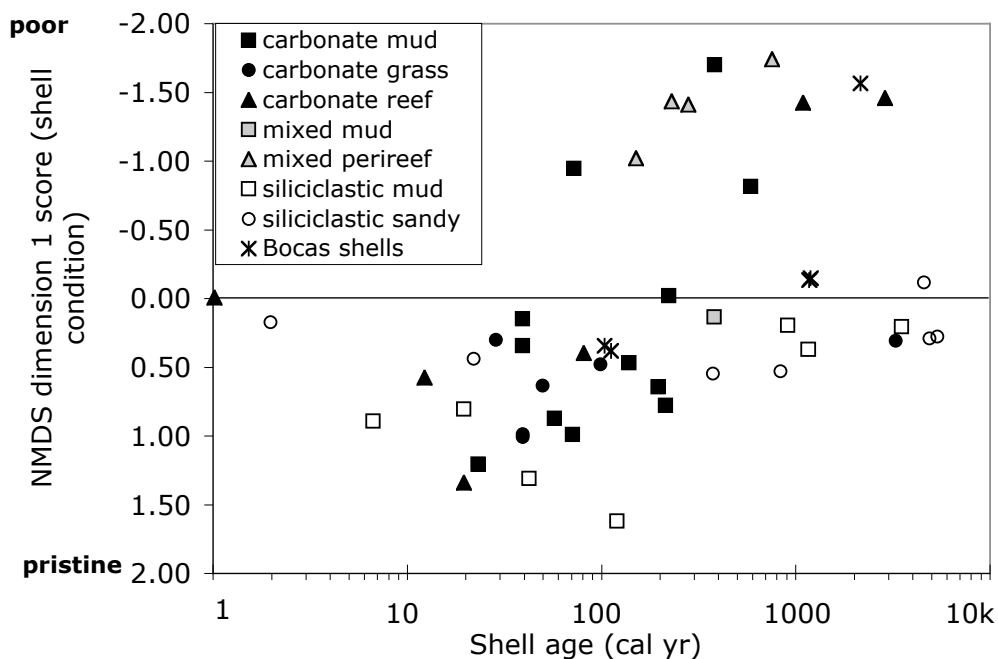


Comments on shell-damage versus age relationship.--All four shells dated from the deeper-water relictual shelf of San Blas are in poor condition (NMDS dimension 1 scores of -0.81 to -1.75; Table DR1). This damage is comparable to that of the oldest carbonate-hosted shells from the modern shelf, and thus would further strengthen the trends apparent among shells from the modern shelf if we were to include them in Figure 2 of the main text. Dates for these 4 shells are based on radiocarbon alone, corrected for reservoir effect; the plot in Figure DR1 indicates that racemization rates on this relictual

shelf are quite different from those of the modern shelf. On the relictual shelf, the 8.6 ka specimen is from an old reef-top, and the other three dated shells (ranging to 15.9 ka) are from a belt of mixed composition sediments. All 4 shells are heavily bored and bio-encrusted.

We also dated 4 *Pitar* specimens from perireefal mixed-composition sediments behind the Zapattillos Cays in Bocas del Toro, along the Caribbean shore of western Panama by applying the San Blas calibration curve to Glu D/L data. These specimens plot within the reefal field established by San Blas specimens (Figure DR5).

Figure DR5. As Figure 2 in the main text, but including 4 dated reefal shells from Bocas del Toro.



Comment on “Accrual of shell damage with post-mortem age”: A method to resegment cohorts?. -- The scatter of values in Figure 2 from the main text (and Figure DR5) indicates that it would be difficult to unambiguously estimate a shell’s age from its state of preservation: the relationship is not significant for siliciclastic/mixed composition

sediments, and significant but low-r among carbonates. However, it might still be possible to segregate the youngest subset by limiting analysis to shells drawn from the “pristine” half of the damage spectrum (whatever that spectrum might be for the material at hand; this would be determined by a preliminary survey). At San Blas, the mid-point of the damage spectrum for carbonates is ~ -0.1 and for siliciclastics $\sim +0.75$; for both sets, shells to the left of the mid-point are all less than 200 years old, a vast improvement in temporal resolution over a random draw from time-averaged assemblages (see Olszewski, 1999 for sampling guides in the absence of information on shell condition).

Subsampling time-averaged assemblages in this manner obviously would not identify all young specimens, only the best preserved ones. Thus the critical issue for transforming this into a practical protocol will be to determine (by intensive dating efforts of multiple species) whether the well-preserved young shells are a random draw from the entire pool of young specimens, and thus provide a reliable sample of taxonomic composition and species’ relative abundances. For application to fully fossil material (versus recent death assemblages), this method assumes that the taphonomic signature of pristine shells survives post-burial processes.

References cited in Appendix 2:

- Denny, M., and Gaines, S., 2000, *Chance in biology: Using probability to explore nature*. Princeton, N.J, Princeton University Press.
- Gumbel, E.J., 1958, *Statistics of extremes*: New York, Columbia University Press.
- Kinnison, R.R., 1985, *Applied extreme value statistics*. Columbus, Ohio : Battelle Press, 149 p.
- Olszewski, T.D., 1999, Taking advantage of time-averaging: *Paleobiology*, v. 25, p. 226-238.
- Staff, G.M., Stanton, R.J., Jr., Powell, E.N., and Cummins, H., 1986, Time-averaging, taphonomy, and their impact on paleocommunity reconstruction: Death assemblage in Texas bays: *Bulletin of the Geological Society of America*, v. 97, p. 428-443.